Dalton Transactions

Accepted Manuscript

This article can be cited before page numbers have been issued, to do this please use: R. J. Marshall, T. Richards, C. Hobday, C. Murphie, C. Wilson, S. Moggach, T. D. Bennett and R. S. Forgan, *Dalton Trans.*, 2015, DOI: 10.1039/C5DT03178H.

This is an *Accepted Manuscript*, which has been through the Royal Society of Chemistry peer review process and has been accepted for publication.

Accepted Manuscripts are published online shortly after acceptance, before technical editing, formatting and proof reading. Using this free service, authors can make their results available to the community, in citable form, before we publish the edited article. We will replace this *Accepted Manuscript* with the edited and formatted *Advance Article* as soon as it is available.

You can find more information about *Accepted Manuscripts* in the Information for Authors.

Please note that technical editing may introduce minor changes to the text and/or graphics, which may alter content. The journal's standard Terms & Conditions and the Ethical guidelines still apply. In no event shall the Royal Society of Chemistry be held responsible for any errors or omissions in this *Accepted Manuscript* or any consequences arising from the use of any information it contains.

ROYAL SOCIETY OF CHEMISTRY

www.rsc.org/dalton

ROYAL SOCIETY OF CHEMISTRY View Article Online
DOI: 10.1039/C5DT03178H

Dalton Transactions

COMMUNICATION

Postsynthetic Bromination of UiO-66 Analogues: Altering Linker Flexibility and Mechanical Compliance†

Received 00th January 20xx,
Accepted 00th January 20xx

DOI: 10.1039/x0xx00000x

www.rsc.org/

Ross J. Marshall,[a] Tom Richards,[b] Claire Hobday,[c] Colin F. Murphie,[a] Claire Wilson,[a] Stephen A. Moggach,[c] Thomas D. Bennett,[b]* and Ross S. Forgan[a]*

A new member of the UiO-66 series of zirconium metal-organic frameworks (MOFs) is reported, and the postsynthetic bromination of its integral alkene moeities in a single-crystal to single-crystal manner is fully characterised. Nanoindentation is used to show bromination of unsaturated carbon-carbon bonds in it and an analogous Zr MOF leads to more compliant materials with lower elastic moduli.

Metal-organic frameworks (MOFs) are network materials comprised of metal ions or clusters connected by organic linkers into multidimensional structures which often exhibit permanent porosity.[1] They have received considerable interest over the last 15 years as a result of their significant potential for application in, for example, gas storage and separation,[2] catalysis,[3] sensing,[4] and drug delivery.[5] The presence of dynamic components, or intrinsic framework flexibility,[6] leads to stimuli-responsive materials[7] which undergo structural changes under applied pressure, temperature or light.[8] Flexibility is often used non-specifically or interchangeably with mechanical compliance, framework elasticity or Young's modulus, *E*, as probed by single crystal nanoindentation. MOFs have been found to possess highly structure-specific values of *E*, which may be useful in sensing, through mechanical response to external stimuli.[9] The nature of both the inorganic node and the organic ligand have been shown to affect *E*, which has also been shown to decrease as framework porosity increases (i.e., more open frameworks are also more compliant).[10] The UiO series of MOFs,[11] which contain $Zr_6O_4(OH)_4$ clusters linked by dicarboxylate ligands, have been predicted to possess significantly larger values of *E* compared to other highly porous MOFs,[12] linker defects notwithstanding.[13] These large elastic moduli, along with large shear and bulk moduli, have been ascribed to the 12-fold coordination of linkers at the Zr^{4+} inorganic node, and indicate significant mechanical rigidity for the UiO isoreticular series. Postsynthetic modification (PSM)[14] has previously been used to exchange metal or ligand functionalities,[15] as well as metallate[16] or covalently modify[17] organic linkers, within the UiO series. We have recently demonstrated (Figures 1a–1c) that the UiO-type MOF $[Zr_6O_4(OH)_4(edb)_6]_n$ (edb = 4,4'-ethynylenedibenzoate),‡ denoted henceforth as **(1)**, can undergo quantitative, stereoselective postsynthetic bromination across the integral alkyne units in a single-crystal to single-crystal (SCSC) manner to form **(1-Br$_2$)**.

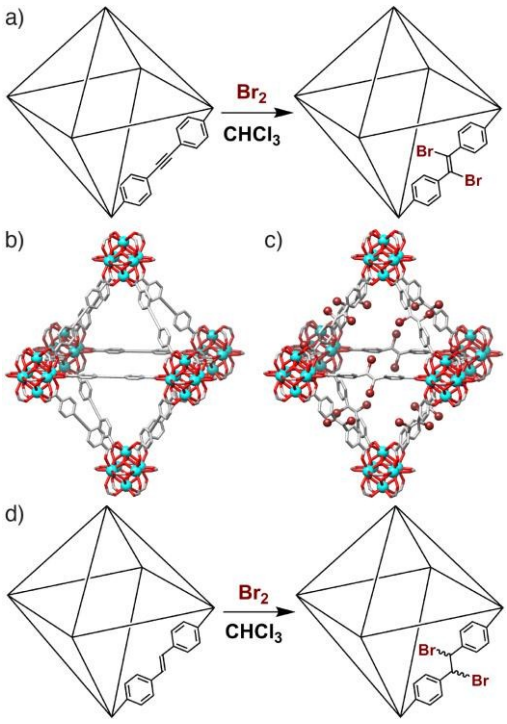

Figure 1. a) Schematic of the bromination of **(1)** to **(1-Br$_2$)**. Representations of the single crystal structures of b) **(1)**, and c) **(1-Br$_2$)**, redrawn from CCDC depositions 1062508 and 1062509, respectively.[18] d) Schematic of the bromination of **(2)** to **(2-Br$_2$)**.

[a] *WestCHEM, School of Chemistry, The University of Glasgow, University Avenue, Glasgow G12 8QQ, UK. E-mail: Ross.Forgan@glasgow.ac.uk*
[b] *Department of Materials Science and Metallurgy, University of Cambridge, Cambridge CB3 0FS, UK. E-mail: tdb35@cam.ac.uk*
[c] *EaStCHEM, School of Chemistry, University of Edinburgh, Joseph Black Building, West Mains Road, Edinburgh, EH9 3JJ, UK.*
†Electronic Supplementary Information (ESI) available: [Synthesis, bromination, characterisation, crystallography and nanoindentation data]. See DOI: 10.1039/x0xx00000x

This results in a contraction of 4% in unit cell volume and a change in hybridisation of the linker carbon atoms from *sp* to sp^2.[18] Herein, we describe the synthesis, characterisation and subsequent SCSC bromination of the analogous alkene containing MOF, $[Zr_6O_4(OH)_4(sdc)_6]_n$ (sdc = 4,4'-stilbene-dicarboxylate, Figure 1d), referred to henceforth as **(2)**, including crystallographic characterisation of the brominated material **(2-Br$_2$)**. Furthermore, we use single crystal nanoindentation to examine the effect of bromination of both **(1)** and **(2)** upon elasticity, or framework compliance.

Bulk samples and single crystals of **(2)**, ≈50 μm in size and suitable for X-ray diffraction (Figure 2a), were prepared using our L-proline modulated procedure (see SI, Section S2). The sdc linker is geometrically frustrated as a result of its non-linearity, leading to end-to-end disorder as seen previously in the crystal structure of **(1-Br$_2$)**.[18] Postsynthetic bromination of alkene units in MOFs has been limited mostly to pendant groups,[19] with the bromination of a Zn MOF containing the sdc linker the only prior example which we are aware of wherein *integral* alkenes are brominated, although the reaction temperature required to induce quantitative conversion (100 °C) appears detrimental to the crystallinity and porosity of the brominated product.[20] In contrast, **(2)** is brominated quantitatively by adding five equivalents of Br_2 per alkene unit to a $CHCl_3$ suspension of **(2)** and soaking for 48 h in the dark at room temperature (see SI, Section S3). NMR spectroscopy of samples of **(2)** and **(2-Br$_2$)** digested in D_2SO_4/DMSO-d_6 was used to ascertain the extent of bromination. Comparison of the ^{1}H NMR spectra of the two digested materials (Figure 2b) shows complete consumption of the starting material during bromination. The characteristic upfield shift of the resonance assigned to the alkene proton confirms quantitative conversion, with the *meso* isomer the predominant product. Similar shifts in the signal for the alkene carbon atoms are observed in the ^{13}C NMR spectra (see SI, Section S4). Minor peaks corresponding to small amounts of a racemic mixture of the diastereomeric products are also visible, unlike the previous report of bromination of a Zn MOF containing the same ligand, which resulted solely in the *meso* isomer.[20]

The porosities of **(2)** and **(2-Br$_2$)** were examined by N_2 adsorption isotherms carried out at 77 K (Figure 2c). BET surface areas decrease from 2900 to 1580 m^2g^{-1} upon bromination of **(2)** in a similar fashion to the values measured for **(1)** and **(1-Br$_2$)**, 3280 and 2000 m^2g^{-1}, respectively.[18] Pore size distributions calculated from the isotherms (see SI, Section S5) show a contraction in the main pore diameter from ≈11.9 Å for **(2)** to ≈10.1 Å for **(2-Br$_2$)**.

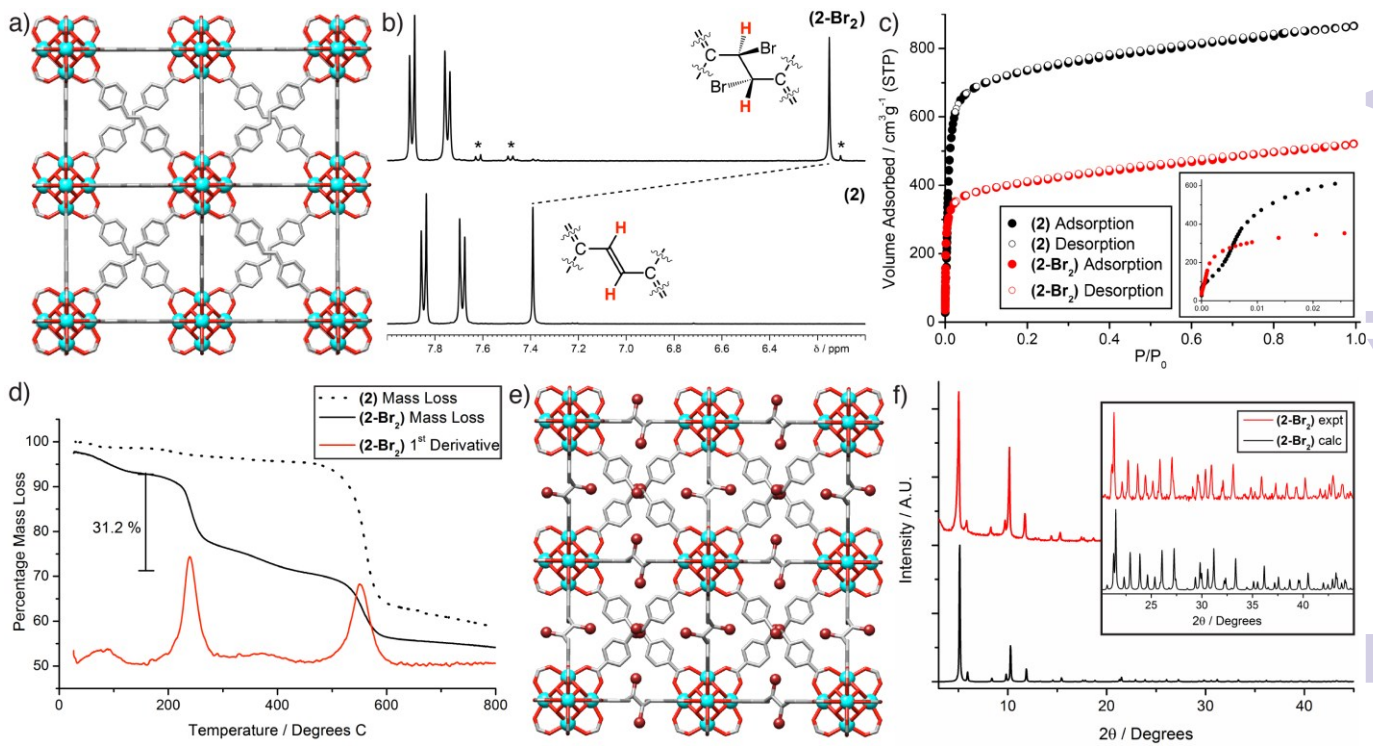

Figure 2. a) Representation of the crystal structure of **(2)** with disorder removed for clarity. b) Stacked ^{1}H NMR spectra (D_2SO_4/DMSO-d_6, 293 K) of digested samples of **(2)** and **(2-Br$_2$)**, showing the *meso* isomer is the major product of bromination. Resonances assigned to the racemic mixture of diastereoisomers are marked with an asterix (*). c) N_2 adsorption isotherms collected at 77 K show a decrease in porosity when **(2)** is brominated to **(2-Br$_2$)**, indicative of a mechanical contraction. d) Thermogravimetric analysis profiles of **(2)** and **(2-Br$_2$)** clearly show the effect of bromination on thermal stability. e) Representation of the crystal structure of **(2-Br$_2$)** with disorder removed for clarity. f) Powder X-ray diffraction analysis of a bulk sample of **(2-Br$_2$)** compared with the pattern calculated from the crystal structure.

These values indicate that bromination lowers the surface area and pore volume as a result of mechanical contraction of the MOFs.§ From the thermogravimetric analysis profiles (Figure 2d), it can be seen that **(2)** exhibits the typical thermal stability

of Zr MOFs, with the large mass loss around 500 °C attributed to combustion of the ligand.[11] In contrast, **(2-Br$_2$)** displays a two-step mass loss profile. Assuming the decrease in mass below 160 °C is desolvation, then the mass loss in the temperature range 160-450 °C accounts for 31.2 % of the mass of the desolvated material; the bromine content of fully evacuated **(2-Br$_2$)** is calculated to be 29.6 %. This very close correlation suggests quantitative bromination of **(2)** has been achieved, supported by a bromine content determined by elemental analysis of 27.7%. The possibility of two mass loss mechanisms – debromination and/or elimination of HBr – may account for the tentative appearance of a very small additional mass loss event around 350-425 °C, but at this point we have been unable to determine whether Br_2 or HBr is being eliminated during the thermal analysis. Elimination of HBr from the evacuated material would result in a mass loss of 30.0 %.

The data collected on the bulk samples all suggest that quantitative bromination has been achieved, and so single crystals of **(2)**, approximately 100 μm in size, were subject to similar bromination conditions (See SI, Section S3) which allowed the isolation of single crystals of **(2-Br$_2$)**. SCSC postsynthetic modification of MOFs,[21] in particular transformations which alter the linker length or geometry,[22] are relatively uncommon. As in the crystal structure of the parent material **(2)** and the related MOF **(1-Br$_2$)**,[18] the ligand in the solid-state structure of **(2-Br$_2$)** is geometrically frustrated, and so there is disorder around the central dibromoethane unit. Despite this, the strongly scattering bromine atoms can be clearly observed (Figure 2e), and the alteration of the ligand geometry is accompanied by a mechanical contraction, with the unit cell edge observed to decrease from 29.8884(3) Å for **(2)** to 29.784(4) Å for **(2-Br$_2$)** as the hybridisation of the central carbon atoms changes from sp^2 to sp^3. This contraction is small, but considering the length of the integral C-C bond has increased during the transformation, this implies that there is a large amount of flexibility at the centre of the ligand. Additionally, the powder X-ray diffraction pattern calculated from the single crystal structure of **(2-Br$_2$)** shows a very close match to the experimental pattern obtained from a bulk brominated sample (Figure 2f). In concert with the other analytical data described previously, it is clear that the bromination of **(2)** is quantitative, and results in a highly crystalline, phase pure material with no detrimental effect on porosity.

The availability of single crystals of ≈50 μm size of all four MOFs enabled nanoindentation to be performed at depths up to 500 nm. The MOFs all display cubic symmetry, and the octahedral crystals were indented on their (111) faces at least 15 times each to derive load-displacement curves (See SI, Section S6). Only one facet was indented due to the octahedral nature of the crystals and their small size. The elastic moduli of **(1)**, **(1-Br$_2$)**, **(2)**, and **(2-Br$_2$)**, extracted from the raw load-displacement data, show the high values of E characteristic[12] of MOFs of the UiO-series (Figure 3). In both cases, bromination results in a decrease in the average elastic modulus of the MOF; from ≈15.1 (± 0.8) GPa to ≈9.3 (± 0.6) GPa as **(1)** is transformed into **(1-Br$_2$)**, and from ≈11.1 (± 0.4) to ≈8.9 (± 0.4) GPa as **(2)** is brominated to **(2-Br$_2$)**. The decrease in overall porosity and solvent accessible volume associated with bromination of the MOFs would normally be expected to *increase* the elastic moduli of the materials.[10]

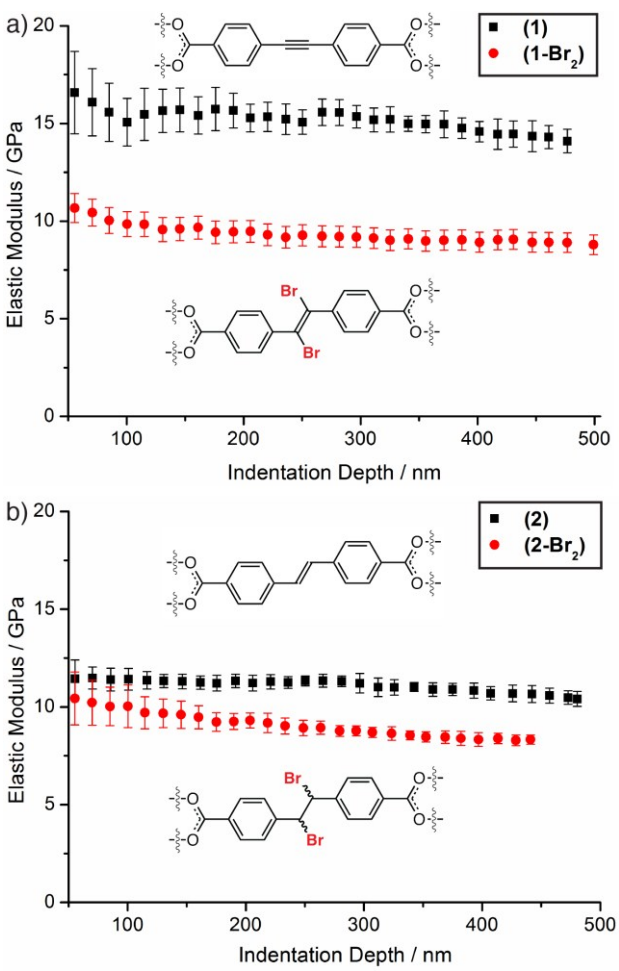

Figure 3. Comparison of elastic moduli as a function of depth for a) **(1)** vs **(1-Br$_2$)** and b) **(2)** vs **(2-Br$_2$)**, showing that bromination results in a reduced elastic modulus in both cases. Error bars are taken from an average of 15 indentations.

Clearly, the generation of more flexible functionality within the linkers impacts significantly on the materials properties of the MOFs. This hypothesis is supported further by the more porous MOF **(1)** having a larger value of E than **(2)**, with the only chemical difference between the two being the hybridisation of the carbon atoms of the central bridge of the linker (sp vs sp^2) and the associated increase in degrees of freedom.

Conclusions

To conclude, we have demonstrated that postsynthetic modification is a powerful tool to induce changes in mechanical properties of MOFs through changes in ligand functionalisation. Generation of sp^2 and sp^3 centres, by

bromination of unsaturated C-C bonds, is facile and quantitative, and the subsequent changes in hybridization significantly impact the elastic moduli of the MOFs. The usefulness of PSM to introduce sp^3 hybridised carbons into otherwise rigid MOFs is further demonstrated by the fact that we have been unable as yet to prepare an isoreticular zirconium MOF using the analogous -CH_2CH_2- bridged ligand, 4,4'-ethane-1,2-diyldibenzoic acid (see SI, Section S7), presumably as a result of its conformational freedom. We anticipate that ligand functionalisation will be a powerful tool to modulate mechanical compliance of MOFs in the future.

Acknowledgements

RSF thanks the Royal Society for receipt of a University Research Fellowship, and the University of Glasgow and EPSRC (EP/L004461/1) for funding. RSF, TDB and SAM gratefully acknowledge pump-priming funding from the EPSRC Directed Assembly Network (PP 14 05 03). TDB thanks Trinity Hall (University of Cambridge) for funding. We thank the EPSRC UK National Crystallographic Service for single crystal data collection for **(2-Br_2)**.[23] The data which underpin this work are available at http://dx.doi.org/10.5525/gla.researchdata.231. CCDC 1418959-1418961 contain the supplementary crystallographic data for this paper. These data can be obtained free of charge from The Cambridge Crystallographic Data Centre via www.ccdc.cam.ac.uk/data_request/cif.

Notes and references

‡The chemical structures of all ligands and their abbreviation scheme used in this study are given in the Supporting Information, in Scheme S1.

§The increase in mass of the brominated MOFs is not sufficient to induce the drastic decreases in gravimetric BET surface areas of **(1-Br_2)** and **(2-Br_2)**.

1 H. Furukawa, K. E. Cordova, M. O'Keeffe and O. M. Yaghi, *Science*, 2013, **341**, 6149.
2 a) E. Barea, C. Montoro and J. A. R. Navarro, *Chem. Soc. Rev.*, 2014, **43**, 5419-5430; b) K. Sumida, D. L. Rogow, J. A. Mason, T. M. McDonald, E. D. Bloch, Z. R. Herm, T.-H. Bae and J. R. Long, *Chem. Rev.*, 2012, **112**, 724-781.
3 a) J. Lee, O. K. Farha, J. Roberts, K. A. Scheidt, S. T. Nguyen and J. T. Hupp, *Chem. Soc. Rev.*, 2009, **38**, 1450-1459;b) J. Gascon, A. Corma, F. Kapteijn and F. X. Llabrés i Xamena, *ACS Catal.*, 2014, **4**, 361-378.
4 L. E. Kreno, K. Leong, O. K. Farha, M. Allendorf, R. P. Van Duyne and J. T. Hupp, *Chem. Rev.*, 2012, **112**, 1105-1125.
5 P. Horcajada, R. Gref, T. Baati, P. K. Allan, G. Maurin, P. Couvreur, G. Férey, R. E. Morris and C. Serre, *Chem. Rev.*, 2012, **112**, 1232-1268.
6 A. Schneemann, V. Bon, I. Schwedler, I. Senkovska, S. Kaskel and R. A. Fischer, *Chem. Soc. Rev.*, 2014, **43**, 6062-6096.
7 F.-X. Coudert, *Chem. Mater.*, 2015, **27**, 1905-1916.
8 G. Férey and C. Serre, *Chem. Soc. Rev.*, 2009, **38**, 1380-1399.
9 J. C. Tan and A. K. Cheetham, *Chem. Soc. Rev.*, 2011, **40**, 1059-1080.
10 a) T. D. Bennett, J.-C. Tan, S. A. Moggach, R. Galvelis, C. Mellot-Draznieks, B. A. Reisner, A. Thirumurugan, D. R. Allan and A. K. Cheetham, *Chem. Eur. J.*, 2010, **16**, 10684-10690; b) J. C. Tan, T. D. Bennett and A. K. Cheetham, *Proc. Natl. Acad. Sci. U.S.A.*, 2010, **107**, 9938-9943.
11 J. H. Cavka, S. Jakobsen, U. Olsbye, N. Guillou, C. Lamberti, S. Bordiga and K. P. Lillerud, *J. Am. Chem. Soc.*, 2008, **130**, 13850-13851.
12 H. Wu, T. Yildirim and W. Zhou, *J. Phys. Chem. Lett.*, 2013, **4**, 925-930.
13 a) H. Wu, Y. S. Chua, V. Krungleviciute, M. Tyagi, P. Chen, T. Yildirim and W. Zhou, *J. Am. Chem. Soc.*, 2013, **135**, 10525-10532; b) M. J. Cliffe, W. Wan, X. Zou, P. A. Chater, A. K. Kleppe, M. G. Tucker, H. Wilhelm, N. P. Funnell, F.-X. Coudert and A. L. Goodwin, *Nat. Commun.*, 2014, **5**, 4176; c) B. Van de Voorde, I. Stassen, B. Bueken, F. Vermoortele, D. De Vos, R. Ameloot, J.-C. Tan and T. D. Bennett, *J. Mat. Chem. A*, 2015, **3**, 1737-1742.
14 S. M. Cohen, *Chem. Rev.*, 2012, **112**, 970-1000.
15 a) M. Kim, J. F. Cahill, H. Fei, K. A. Prather and S. M. Cohen, *J. Am. Chem. Soc.*, 2012, **134**, 18082-18088; b) H. Fei and S. M. Cohen, *J. Am. Chem. Soc.*, 2015, **137**, 2191-2194.
16 a) M. I. Gonzalez, E. D. Bloch, J. A. Mason, S. J. Teat and J. R. Long, *Inorg. Chem.*, 2015, **54**, 2995-3005; b) K. Manna, T. Zhang, F. X. Greene and W. Lin, *J. Am. Chem. Soc.*, 2015, **137**, 2665-2673.
17 a) S. J. Garibay and S. M. Cohen, *Chem. Commun.*, 2010, **46**, 7700-7702; b) M. Kandiah, S. Usseglio, S. Svelle, U. Olsbye, K. P. Lillerud and M. Tilset, *J. Mater. Chem.*, 2010, **20**, 9848-9851; c) W. Morris, W. E. Briley, E. Auyeung, M. D. Cabezas and C. A. Mirkin, *J. Am. Chem. Soc.*, 2014, **136**, 7261-7264.
18 R. J. Marshall, S. L. Griffin, C. Wilson and R. S. Forgan, *J. Am. Chem. Soc.*, 2015, **137**, 9527-9530.
19 a) K. Hindelang, A. Kronast, S. I. Vagin and B. Rieger, *Chem. Eur. J.*, 2013, **19**, 8244-8252; b) T. K. Prasad and M. P. Suh, *Chem. Eur. J.*, 2012, **18**, 8673-8680; c) F. Sun, Z. Yin, Q.-Q. Wang, D. Sun, M.-H. Zeng and M. Kurmoo, *Angew. Chem. Int. Ed.*, 2013, **52**, 4538-4543; d) Z. Wang and S. M. Cohen, *Angew. Chem. Int. Ed.*, 2008, **47**, 4699-4702.
20 S. C. Jones and C. A. Bauer, *J. Am. Chem. Soc.*, 2009, **131**, 12516-12517.
21 J. -P. Zhang, P. -Q. Liao, H. -L. Zhou, R. -B. Lin and X. -M. Chen, *Chem. Soc. Rev.*, 2014, **43**, 5789-5814.
22 P. –Q. Liao, A. -X Zhu, W. –X. Zhang, J. –P. Zhang and X. –M. Chen, *Nat. Commun.*, 2015, **6**, 6350.
23 S. J. Coles and P. A. Gale, *Chem. Sci.*, 2012, **3**, 683-689.

View Article Online
DOI: 10.1039/C5DT03178H

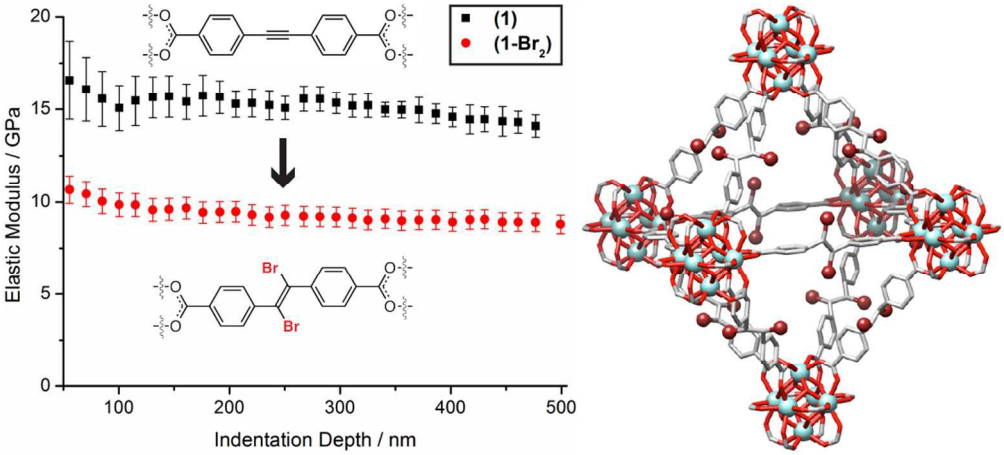

99x44mm (300 x 300 DPI)